Dual-Mode Chest Wearable E-Tattoo for the Mobile Detection of Cardiac Time Intervals

Sarnab Bhattacharya
University of Texas at Austin
Austin, Texas, USA

Mohammad Nikbakht
Georgia Institute of Technology
Atlanta, USA

Alec Alden
University of Texas at Austin
Austin, Texas, USA

Karina Ambani
University of Texas at Austin
Austin, Texas, USA

Philip Tan
University of Texas at Austin
Austin, Texas, USA

Taha A Alhalimi
University of Texas at Austin
Austin, Texas, USA

Jieting Wang
University of Texas at Austin
Austin, Texas, USA

Hirofumi Tanaka
University of Texas at Austin
Austin, Texas, USA

Edward F Coyle
University of Texas at Austin
Austin, Texas, USA

Omer Inan
Georgia Institute of Technology
Atlanta, USA

Nanshu Lu*
University of Texas at Austin
Austin, Texas, USA
nanshulu@utexas.edu

ABSTRACT

Ambulatory cardiovascular monitoring could be vital for pre-emptive detection of heart disease and timely intervention to prevent serious cardiac complications. In this work we present a thin, flexible, stretchable, ultra light-weight wireless cardiac monitoring device that can be laminated onto the human chest like a temporary tattoo, called the e-tattoo. The e-tattoo laminated on human chest is able to extract important cardiac event and systolic timing intervals (STI) via dual-mode electrocardiography (ECG) and seismocardiography (SCG) sensors. The light, conformal form factor coupled with low power consumption enables uninterrupted monitoring of important STI like pre-ejection period (PEP) and left ventricular ejection time (LVET) over extended periods of time. We have achieved preliminary validation of the device against gold standards on a human subject.

CCS CONCEPTS

• **Applied computing** → **Life and medical sciences**; • **Hardware** → *Emerging technologies.*

KEYWORDS

Electrocardiogram, seismocardiogram, systolic timing intervals.

*Corresponding author

CHASE' 22, November 17–19, 2022, Washington, DC, USA

ACM ISBN 978-1-4503-9476-5/22/11…$15.00
https://doi.org/10.1145/3551455.3559607

ACM Reference Format:
Sarnab Bhattacharya, Mohammad Nikbakht, Alec Alden, Karina Ambani, Philip Tan, Taha A Alhalimi, Jieting Wang, Hirofumi Tanaka, Edward F Coyle, Omer Inan, and Nanshu Lu. 2022. Dual-Mode Chest Wearable E-Tattoo for the Mobile Detection of Cardiac Time Intervals. In *ACM/IEEE International Conference on Connected Health: Applications, Systems and Engineering Technologies (CHASE' 22), November 17–19, 2022, Washington, DC, USA.* ACM, New York, NY, USA, 5 pages. https://doi.org/10.1145/3551455.3559607

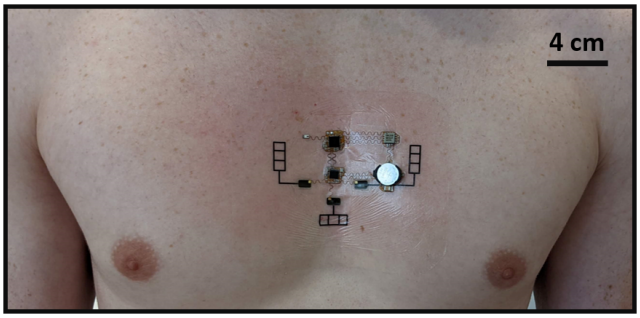

Figure 1: The presented lightweight, chest laminated ECG and SCG sensing system consisting of custom electronics pattern in a stretchable design along with bio-compatible carbon film electrodes

1 INTRODUCTION

Cardiovascular health is considered an essential aspect of overall human health. When the heart stops, essential bodily functions fail, some almost instantly. *"Heart disease is the leading cause of death for men, women and people of most ethnic groups in the United States"* according to the Center for Disease Control and Prevention (CDC). The ability to continuously monitor cardiovascular parameters is

critical in being able to provide quality healthcare to individuals who may require timely intervention to prevent cardiovascular dysfunction.

The cardiac cycle consists of four phases—isovolumetric contraction, systolic ejection, isovolumetric relaxation, and diastolic filling. Of these, isovolumetric contraction and systolic ejection are of particular interest. The period of the isovolumetric contraction is the time between the electrical excitation of the ventricular cardiomyocytes (Q on the ECG) and the opening of the aortic valve (AO). This interval is also known as the pre-ejection period (PEP) and is a surrogate for the myocardial contractility [6]. The period of the systolic ejection is also known as the left ventricular ejection time (LVET) and is the time from the end of isovolumetric contraction to the closure of the aortic valve (AC). The sum of these two periods (QS_2) is the total time the hearts spends in ventricular systole and is an important cardiac parameter. PEP and LVET are also closely tied with heart failure. A lengthening of the PEP and a shortening of the LVET while QS_2 intervals are normal was found in people suffering from heart failure [11]. It has been proposed that the ratio between PEP and LVET is a good indicator of left ventricular (LV) dysfunction[1].

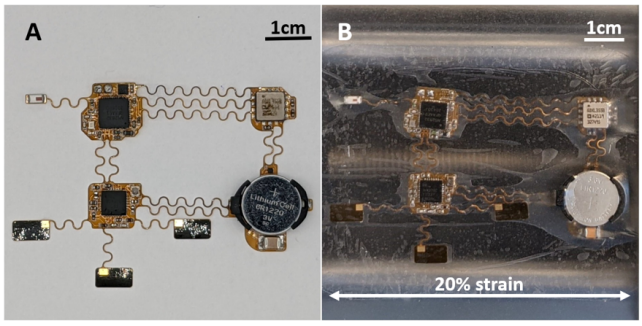

Figure 2: (A) The electronic design of the device with specific components segregated into different islands with serpentine interconnect in between. (B) The device laminated in medical dressing being stretched up to 20% of original length.

The de-facto widely used method of gauging cardiovascular health is using an Electrocardiogram (ECG). Though it is an important tool in monitoring cardiovascular health, its main drawback is that it only senses the electrical activity of the heart and is not able to provide any information about the mechano-acoustic activity of the heart including contraction, valve activity and blood flow. Researchers have looked into various non-invasive methods to capture these mechano-acoustic aspects of the cardiovascular system. Impedance cardiography (ICG) devices measure the blood flow in the thorax. Blood being pumped by the heart causes changes in the thoracic impedance which can be correlated to different cardiac events. In healthy subjects with low body mass index (BMI), this technique can provide accurate measures of some systolic timing intervals (STIs); however, in broader populations with cardiovascular diseases, and in patients with higher BMI the method has shown to have high error compared to reference standard invasive measures [7, 8]. Phonocardiograms (PCG) captures the acoustic signals generated by the heart valves. However, PCG measures the *closure* of the valves rather than the opening, and thus cannot provide an indication of the opening of the aortic valve as needed for both PEP and LVET. More recently ballistocardiogram (BCG) and seismocardiogram (SCG) measurements have become popular for mechanical heart function assessments [5]. The BCG signal is the whole body motion due to the ejection of blood by the heart and movement of blood through the vasculature. The SCG signal is a more localised measurement of the chest vibrations associated with cardiac contraction and blood movement, usually measured at or near the sternum.

A non-invasive, low cost, unobtrusive and accurate method to monitor these STIs would be beneficial not only to hospitalized patients for reducing the cost of healthcare, but can also be used by the general at risk population for ambulatory monitoring of cardiac function at home.

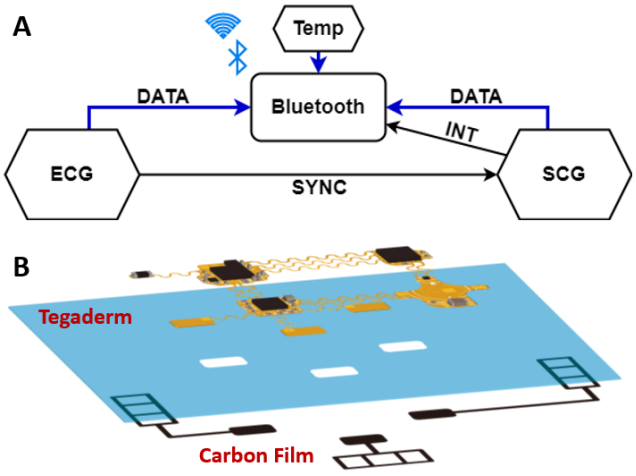

Figure 3: (A) Block diagram of the system electronics. (B) Device stack-up showing exploded view of the electrodes assembled together with the electronics and medical dressing.

In this paper we propose an innovative stretchable, thin, ultra-lightweight, dual mode ECG-SCG wireless monitoring device that can be attached to the human chest like a temporary sticker as shown in Fig. 1. The stretchable, flexible and thin form factor conforms to the human chest, and the lightweight design allows for improved mechanical coupling and SCG signal quality. Recordings are transmitted in real-time over Bluetooth to a central device for processing. A signal processing algorithm was designed to extract ECG and SCG features to calculate PEP and LVET on the central device. The major contributions of this work are:

- A flexible, stretchable device that is maximally conformable to human skin to enable unobtrusive cardiac monitoring.
- System design to optimize for low power while enabling robust measurement of the cardiac parameters.

We validate our system on a human subject against echocardiogram measurements as well as a clinical cardiac monitor.

2 METHODS

2.1 Hardware

The circuit was fabricated on commercial flexible printed circuit board (FPC) material, which consists of a polyimide substrate with copper layers on top and bottom. The total thickness of the FPC is 100um. Electronic components corresponding to a specific functions are segregated into physical islands that are connected by serpentine interconnects. The serpentine interconnects allow the circuit to stretch up to 20% without causing any damage to the electronics (Fig. 2). The whole device including electronics, battery, electrodes and medical dressing weighs less than 2.5g.

2.1.1 Sensors. For our central processing unit (CPU) we have used the Nordic nRF52832 Bluetooth low-energy (BLE) transceiver. For the ECG sensor the MAX30003 chip from Maxim Integrated was used. It offers a single lead ECG with right leg drive. The electrodes are manufactured by laser cutting 50um thick carbon film into a specific pattern and transferring it onto medical dressing (Tegaderm, 3M). Tegaderm has an elastic modulus that is very close to that of human skin. Holes are cut on the Tegaderm to expose parts of the electrodes which were connected to the electronics using pressure activated, anisotropic conductive tape (Fig. 3B).

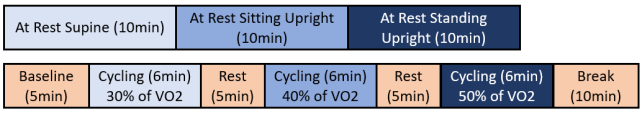

Figure 4: Protocol followed during the human subject experiments. This protocol was approved by the Institutional Review Board (IRB)

The SCG sensor is a highly sensitive 3-axis accelerometer (ADXL-355) from Analog Devices with a noise floor of $25\mu g/\sqrt{(Hz)}$ and a resolution of $3.9\mu g$ ($1g = 9.8m/s^2$). Frequencies up to 40Hz were captured with the sensor. Frequency components in the 1-40Hz range captured the chest vibrations when the subject is at rest. The 0.2-1Hz range captured mainly the chest motion due to respiration. Finally the DC frequency component provided information on the relative orientation of the subject.

In addition a temperature sensor (TMP117) from Texas Instruments, with an accuracy of $\pm 0.1^{\circ}C$, is mounted on the underside of the BLE island to be in close contact with the human body to capture central skin temperature. The ECG and SCG signals were sampled at 125Hz and the temperature sensor was sampled at 1Hz. In post processing the ECG and SCG signals were up-sampled to 1KHz to increase temporal resolution.

2.1.2 Synchronisation. In this study we focused on PEP and LVET. To obtain PEP it is imperative that the synchronisation between sampling instances of the ECG and the SCG sensor be very accurate. However the MAX30003 and ADXL355 run on their own local clock. When sampling over a long duration, we observed clock drift. To mitigate this we use the scheme of peripheral-to-peripheral communication to facilitate high fidelity synchronisation while also reducing system power consumption. The ECG sensor generates a *sync* pulse on every sampling event. The SCG sensor begins sampling on the rising edge of this signal. On both the ECG and SCG sensor the recorded samples are pushed into a FIFO. During the time that the FIFO is getting filled, the CPU is in a low power sleep mode. When the FIFO fills up to a set level the SCG sensor generates an interrupt which wakes the CPU from its sleep state. This is illustrated in Fig. 3A. The data is then read from both the sensors, compressed into a compact packet, and then transmitted over BLE to a host device for post-processing.

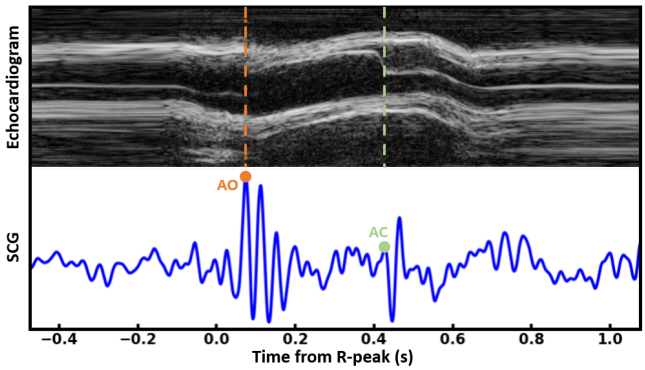

Figure 5: Synchronised M-mode echocardiogram and SCG signal with aortic valve opening marked in orange and aortic valve closing marked in green

2.1.3 Power Consumption. The MAX30003 generates single channel 18 bit wide ECG data, and the ADXL355 generates 3 channel (X,Y and Z) 20 bits wide data. For simplicity we assign 3 bytes to each channel making the total sample size 12 bytes. We use the extended BLE packet mode where each BLE packet can carry 244 bytes of data enabling transmission of 20 samples per packet. The remaining 4 bytes are used to transmit temperature (2 bytes) and an internal timestamp (2 bytes) to check for packet drops. We use the maximum possible packet size to efficiently transmit data and reduce overall system power consumption due to data transmission and also to keep the CPU in sleep mode longer. To further optimize power consumption we have enabled the on chip buck converter on the nRF52832 which supplies the BLE radio. With all these power optimisation methods our overall system power draw is 0.9mA. We use a small form factor coin cell battery (CR1220) that is able to power our device for over 25 hours. Our goal was to make our device ultra-lightweight and thus we chose to use this particular battery which weighs only 750 mg. Although the average current consumption is low, during BLE data transmission, the current draw can rise up to 15 mA for a very short duration causing damage to the battery and reducing its expected capacity. To mitigate this we have added a R-C passive low pass filter between the battery and the electronics to smooth out these current spikes.

2.2 Data Processing

From the SCG recordings, z-axis acceleration data (dorso-ventral axis) was used for the purpose of this study. The z-axis of the SCG signal has shown to contain the main components of the SCG signal [5]. Since the SCG signals are small signals in nature,

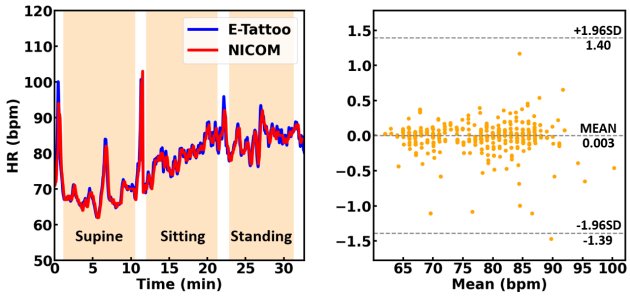

Figure 6: HR plotted with time for various static postures comparing the device data with NICOM (left). Bland Altman comparison of device data with the NICOM data (right)

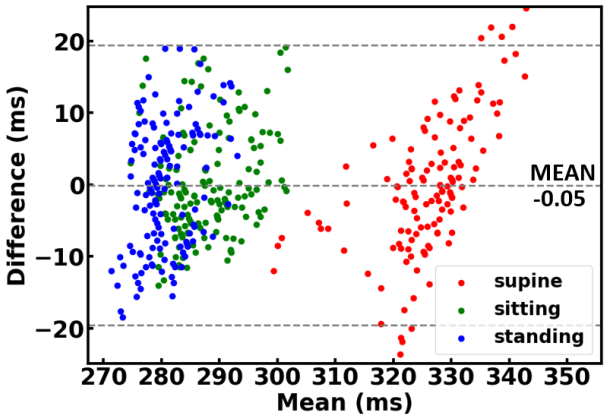

Figure 7: LVET data from E-tattoo compared with NICOM during static posture trial. Red corresponds to supine, green with upright sitting and blue with standing.

motion noise may dominate causing the feature extraction to fail. To address this we only use rest periods for feature extraction. The rest periods contain less motion noise compared to the activity segments, while containing important recovery information after any activity segments. Next, The signals were filtered using a Butterworth filter with cutoff frequencies of 1-40 Hz [9]. After filtering, we extracted the R-peaks of the ECG signals that were collected along with the SCG signals. Using the R-peaks, the SCG signals were segmented into SCG beats starting from the occurrence of the R-peak to 500 ms after the R-peak to make sure it contains all of the clinically relevant components of the SCG beat.

To calculate PEP and LVET features of the SCG beats, we need to extract AO and AC locations from the SCG beats. For this, a causal peak tracking method was used to extract AO and AC features from the segmented beats [4]. Finally, the PEP, and LVET parameters were calculated using the extracted features and compared with the gold standard measurements.

2.3 Validation

To validate our hardware and software components, we conducted 2 human subject experiments under an Institutional Review Board (IRB) approved protocol at the University of Texas at Austin with IRB ID STUDY00002313. Informed consents were obtained from all subjects involved in the study. First we performed simultaneous measurements with our e-tattoo and an echocardiogram to confirm the accuracy of our system in being able to extract PEP and LVET values. This experiment also allowed us to correlate cardiac events to features from the SCG signal and validate our SCG sensor's ability to precisely sense these minute vibrations. M-mode echocardiography was performed on a subject who also had the e-tattoo attached for a duration of 2 minutes, capturing 115 heart beats. The echocardiogram and SCG signals were synchronised using their corresponding ECG signals to allow comparison of the two.

For the second experiment, the participant went through a protocol consisting of holding static poses and performing cycling under incremental load while wearing our device along with a non-invasive cardiac output monitor (NICOM) for getting ground truth. The NICOM is an FDA cleared hemodynamic monitoring which uses bio-reactance to measure thoracic blood flow. Changing the body orientation induces small changes in STIs, while cycling induces large changes in STIs. The flow of this experiment is illustrated in Fig. 4. Prior to this experiment the participant underwent a VO_2 max test so that the load on the cycle ergometer could be set to specific values based on the participants oxygen uptake limits. From the synchronous NICOM measurements we were able to obtain HR and LVET parameters to validate the recordings from our device. Note that the NICOM does not provide PEP values.

3 RESULTS

Figure 5 shows the echocardiogram signals with the corresponding synchronized SCG signal obtained from the first experiment. The SCG signal has two major high energy segments corresponding to the first and second heart sound. The AO corresponds to the first major peak of the first segment, and the AC is near the beginning of the first major minima of the second segment. This is in line with finding of previous literature [2, 10]. Using our algorithm to extract PEP and LVET, there was an error of 3.8% for PEP and 3.2% for LVET compared to the echocardiogram data averaged across all beats. We also compared LVET from the NICOM device, which we used for the second experiment, to the echocardiogram data. Interestingly we observed that the NICOM was under-reporting LVET values. This is because the features on the ICG waveform do not correspond well with actual cardiac events as is demonstrated by Dehkordi et al.[3]. However if the NICOM value was scaled by a fixed value, obtained via regression fitting with the echocardiogram data, then the results were comparable. We use this scaled NICOM value to compare with our device recordings.

For the static poses, the HR (reported in beats per minute) from our device and from the NICOM was highly correlated as shown in Fig. 6. Performing the Bland Altman analysis shows the mean difference is only 0.003 bpm with a standard deviation of 0.71 bpm. PEP during the supine, upright sitting and standing posture was 91.35 ms, 97.7 ms and 100.3 ms respectively and remained fairly unchanging. These values are close to what is expected from a healthy adult, but as mentioned in section 2.3 there was no gold standard to validate it against. Fig. 7 shows the variation in LVET during the different poses as well as the difference when compared

to the NICOM data. The mean difference across all static postures was -0.05 ms with a standard deviation of 9.94 ms. The higher average LVET during supine posture can be attributed to a higher cardiac preload in the supine posture.

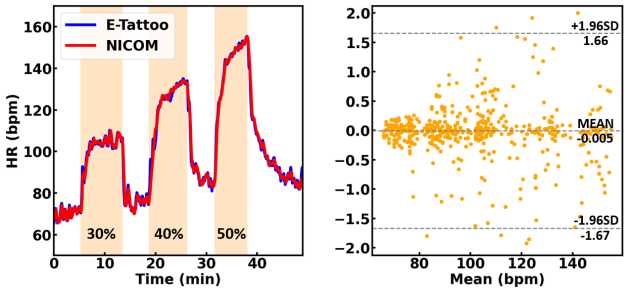

Figure 8: HR plotted with time during the incremental load cycling experiment (left). Bland Altman comparison of device data with the NICOM data (right)

The second part of the protocol was to induce a large change in STIs. Incremental cycling at moderate loads was able to vary HR up to 155 bpm. STIs were extracted during the rest periods as mentioned before. Even during excessive motion while cycling, our system was able to extract very accurate HR using the ECG recordings as shown in Fig. 8. A similar Bland Altman analysis of the HR yielded a mean difference of -0.005 bpm from the NICOM and a standard deviation of 0.85 bpm. The variation in LVET was more pronounced during this experiment with the lowest value being 177 ms. Fig. 9 compares the LVET extracted from the device measurements with the LVET measured by the NICOM, showing a mean difference at -1.78 ms and a standard deviation of 9.24 ms.

These results demonstrate that the error in measuring HR and LVET with our device is small compared to a clinically approved gold standard, making our device a viable alternative to these bulky and obtrusive methods.

4 CONCLUSION

Our device presents an unobtrusive and comfortable solution to perform ambulatory cardiac monitoring of STIs. Validating our device against echocardiogram has demonstrated high accuracy in detecting important STIs. Testing on one subject has demonstrated the accuracy of tracking HR and LVET over a substantial range of HR. Future work will focus on long term wearability trials, as well as an in-depth characterisation of the mechanical robustness of our conformal sensor. Lastly future work can also explore estimation of higher order cardiac parameters such as stroke volume and ejection fraction from the device recordings using machine learning techniques.

ACKNOWLEDGMENTS

This research is sponsored by the US Office of Naval Research under the Grant No. N00014-20-1-2112, and the National Science Foundation under the Grant No. 2133106. OTI[1] is supported by the Linda J. and Mark C. Smith Chair funds at Georgia Tech.

[1] *Disclosures*: OTI is a co-founder and board member of Cardiosense, Inc.

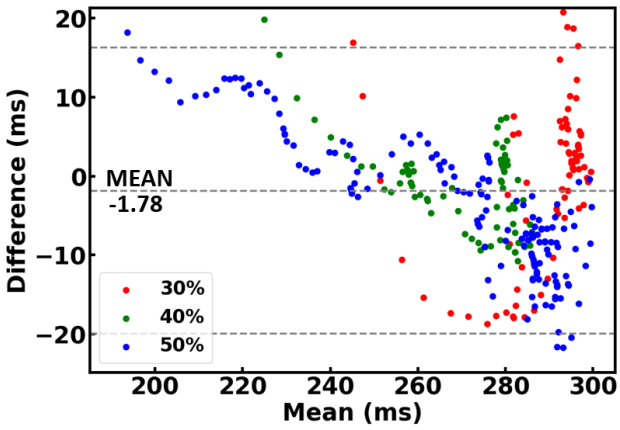

Figure 9: LVET data from E-tattoo compared with NICOM during recovery after cycling. Red , green and blue correspond to increasing load while cycling.

REFERENCES

[1] H Boudoulas. 1990. Systolic time intervals. *European heart journal* 11, suppl_I (1990), 93–104.

[2] Richard S Crow, Peter Hannan, David Jacobs, Lowell Hedquist, and David M Salerno. 1994. Relationship between seismocardiogram and echocardiogram for events in the cardiac cycle. *American journal of noninvasive cardiology* 8 (1994), 39–46.

[3] Parastoo Dehkordi, Farzad Khosrow-Khavar, Marco Di Rienzo, Omer T Inan, Samuel E Schmidt, Andrew P Blaber, Kasper Sørensen, Johannes J Struijk, Vahid Zakeri, Prospero Lombardi, et al. 2019. Comparison of different methods for estimating cardiac timings: a comprehensive multimodal echocardiography investigation. *Frontiers in physiology* (2019), 1057.

[4] Asim H Gazi, Srirakshaa Sundararaj, Anna B Harrison, Nil Z Gurel, Matthew T Wittbrodt, Mhmtjamil Alkhalaf, Majd Soudan, Oleksiy Levantsevych, Ammer Haffar, Amit J Shah, et al. 2021. Transcutaneous Cervical Vagus Nerve Stimulation Inhibits the Reciprocal of the Pulse Transit Time's Responses to Traumatic Stress in Posttraumatic Stress Disorder. In *43rd Annual International Conference of the IEEE Engineering in Medicine & Biology Society (EMBC)*. 1444–1447.

[5] Omer T Inan, Pierre-Francois Migeotte, Kwang-Suk Park, Mozziyar Etemadi, Kouhyar Tavakolian, Ramon Casanella, John Zanetti, Jens Tank, Irina Funtova, G Kim Prisk, et al. 2014. Ballistocardiography and seismocardiography: A review of recent advances. *IEEE journal of biomedical and health informatics* 19, 4 (2014), 1414–1427.

[6] Richard P Lewis, SE Rittogers, WF Froester, and H Boudoulas. 1977. A critical review of the systolic time intervals. *Circulation* 56, 2 (1977), 146–158.

[7] Angela Quain, Mark Hoyer, Georges Ephrem, and W Aaron Kay. 2021. Non-invasive cardiac output monitoring (NICOM) in adult congenital heart disease patients with Fontan palliation. *International Journal of Cardiology Congenital Heart Disease* 6 (2021), 100287.

[8] Aniket Rali, Tyler Buechler, Bridget Van-Gotten, Emily Burgen, John Chen, Zubair Shah, Nicholas Haglund, and Andrew Sauer. 2019. DOES NON-INVASIVE CARDIAC OUTPUT MONITORING (NICOM) CORRELATE WITH STANDARD INVASIVE HEMODYNAMIC MONITORING IN PATIENTS WITH ACUTE DECOMPENSATED HEART FAILURE? *Journal of the American College of Cardiology* 73, 9S1 (2019), 819–819.

[9] Md Mobashir Hasan Shandhi, Beren Semiz, Sinan Hersek, Nazli Goller, Farrokh Ayazi, and Omer T Inan. 2019. Performance analysis of gyroscope and accelerometer sensors for seismocardiography-based wearable pre-ejection period estimation. *IEEE journal of biomedical and health informatics* 23, 6 (2019), 2365–2374.

[10] Kasper Sørensen, Samuel E Schmidt, Ask S Jensen, Peter Søgaard, and Johannes J Struijk. 2018. Definition of fiducial points in the normal seismocardiogram. *Scientific reports* 8, 1 (2018), 1–11.

[11] Arnold M Weissler, Willard S Harris, and Clyde D Schoenfeld. 1968. Systolic time intervals in heart failure in man. *Circulation* 37, 2 (1968), 149–159.